View metadata, citation and similar papers at core.ac.uk
brought to you by CORE
provided by Elsevier - Publisher Connector

Neuron, Vol. 23, 33–44, May, 1999, Copyright ©1999 by Cell Press

Alternatively Spliced Isoforms of Nerve- and Muscle-Derived Agrin: Their Roles at the Neuromuscular Junction

Robert W. Burgess, Quyen T. Nguyen,
Young-Jin Son, Jeff W. Lichtman,
and Joshua R. Sanes*
Department of Anatomy and Neurobiology
Washington University Medical School
St. Louis, Missouri 63110

Summary

Agrin induces synaptic differentiation at the skeletal neuromuscular junction (NMJ); both pre- and postsynaptic differentiation are drastically impaired in its absence. Multiple alternatively spliced forms of agrin that differ in binding characteristics and bioactivity are synthesized by nerve and muscle cells. We used surgical chimeras, isoform-specific mutant mice, and nerve–muscle cocultures to determine the origins and nature of the agrin required for synaptogenesis. We show that agrin containing Z exons (Z^+) is a critical nerve-derived inducer of postsynaptic differentiation, whereas neural isoforms containing a heparin binding site (Y^+) and all muscle-derived isoforms are dispensable for major steps in synaptogenesis. Our results also suggest that the requirement of agrin for presynaptic differentiation is mediated indirectly by its ability to promote postsynaptic production or localization of appropriate retrograde signals.

Introduction

Formation of chemical synapses requires a complex interchange of signals between the pre- and postsynaptic partners. At the skeletal neuromuscular junction (NMJ), where this interchange has been studied in detail, agrin is a critical organizer of postsynaptic differentiation (reviewed by McMahan, 1990; Bowe and Fallon, 1995; Sanes and Lichtman, 1999). Agrin is a heparan sulfate proteoglycan that was purified on the basis of its ability to cause aggregation (hence the name) of diffusely distributed acetylcholine receptors (AChRs) on the surface of cultured myotubes. Subsequent studies showed that agrin also induces the aggregation of numerous other proteins that are concentrated in the membrane, matrix, and cytoskeleton of the postsynaptic apparatus. Agrin synthesized by motoneurons is transported along their axons and released into the synaptic cleft, where it becomes stably associated with the basal lamina. Together, these observations led McMahan and colleagues (1992) to propose the "agrin hypothesis," which states that agrin is a critical nerve-derived organizer of postsynaptic differentiation. In support of this hypothesis, focal expression of recombinant agrin in muscle fibers results in the assembly of a virtually complete but aneural postsynaptic apparatus (Cohen et al., 1997a; Jones et al., 1997; Meier et al., 1997; Rimer et al., 1997), and synaptic differentiation is profoundly impaired in agrin-deficient "knockout" mice (Gautam et al., 1996).

Although the *agrin* mutant proved that agrin is necessary for neuromuscular synaptogenesis in vivo, it left several important issues unresolved. First, although agrin is synthesized by motoneurons and concentrated in the synaptic cleft of adult NMJs, it is also expressed by developing myotubes and Schwann cells and is present throughout their basal laminae in embryos (Godfrey et al., 1988; Fallon and Gelfman, 1989; Hoch et al., 1993; Halfter et al., 1997; see Figure 1). This broad distribution initially raised doubts about the ability of agrin to mediate the effects of nerve on muscle, but it was later shown that alternatively spliced forms of agrin expressed by neurons are more active than those expressed by muscle. In particular, isoforms with insertions of 8, 11, or 19 (11 + 8) amino acids at a site called B in chicks and Z in mammals (collectively called Z^+ agrin here) are expressed by motoneurons but not by myotubes and are 100- to 1000-fold more potent in AChR clustering assays than forms lacking these inserts (Z^- agrin) (Ferns et al., 1992, 1993; McMahan et al., 1992; Ruegg et al., 1992; Gesemann et al., 1995). Thus, it is plausible that the nerve-derived Z^+ agrin is a synaptic organizing molecule, and Z^- isoforms play other roles. However, even Z^- agrin has some AChR clustering activity (Campanelli et al., 1991; Ferns et al., 1992), so this hypothesis is far from proven. Because the original allele (called $agrn^{neo/neo}$ here) affected all forms of agrin, it was not possible to distinguish roles of Z^- and Z^+ agrin.

A second unresolved issue is whether agrin directly promotes pre- as well as postsynaptic differentiation. In normal mice, motor axons leave the intramuscular nerve, induce postsynaptic sites, and differentiate there into nerve terminals. In the $agrn^{neo/neo}$ mutants, in contrast, axons leaving the intramuscular nerve run long distances parallel to myotubes and form few terminal arbors. These abnormalities could be either direct or indirect consequences of agrin deficiency. That is, in the absence of agrin, the postsynaptic apparatus might fail to synthesize or localize retrograde factors necessary to stop motor axonal growth and promote motor nerve terminal differentiation. Alternatively, agrin itself might inhibit growth or promote presynaptic differentiation. In support of the second alternative, Campagna et al. (1995, 1997) and Chang et al. (1997) have shown that recombinant agrin can serve as a stop signal for motor axons and can promote the clustering of synaptic vesicles within axons. Z^+ agrin and Z^- agrin affected neurites with equal potency in these experiments, suggesting that muscle as well as nerve agrin might affect motor axons in vivo. In fact, it is even possible that postsynaptic defects in the mutant are secondary to presynaptic defects; if muscle agrin is essential for presynaptic differentiation, then motor axons in $agrn^{neo/neo}$ mice might be unable to provide anterograde signals—which might or might not include agrin—that trigger postsynaptic differentiation. Although this scenario seems

*To whom correspondence should be addressed (e-mail: sanesj@thalamus.wustl.edu).

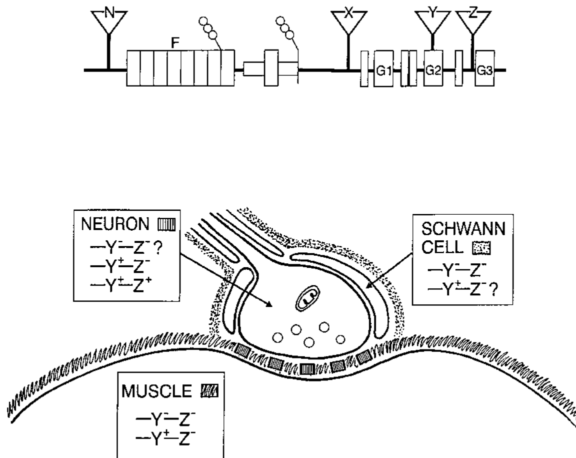

Figure 1. Sources and Isoforms of Agrin

Although agrin is selectively associated with synaptic basal lamina in adult muscle, it is present throughout the basal lamina in embryos. The agrin is synthesized by neurons, myotubes, and Schwann cells. Only neurons synthesize forms that contain inserts at the alternatively spliced Z site. All Z^{+} forms also contain an insert at the Y site, but some Y^{+} forms are Z^{-}. Both muscle and nerve synthesize $Y^{+}Z^{-}$ and $Y^{-}Z^{-}$ forms. The Y insert is necessary for heparin binding, and the Z inserts dramatically enhance AChR clustering activity. Our results indicate that only Z^{+} agrin is required for synaptogenesis.

unlikely, results from the agrin mutant are compatible with it.

Third, agrin is alternatively spliced not only at the Z site but also at a site called A in chick and Y in mammals. Recombinant Z^{+} agrin molecules that contain a four amino acid insert at the Y site (Y^{+}) are severalfold more potent at clustering AChRs on cultured myotubes than the corresponding $Y^{-}Z^{+}$ forms, suggesting that the Y insert modulates agrin signaling (Ruegg et al., 1992; Ferns et al., 1993; Campanelli et al., 1996; Gesemann et al., 1996). Moreover, inclusion of the Y insert endows agrin with the ability to bind heparin and, by implication, heparan sulfate proteoglycans (Campanelli et al., 1996; Gesemann et al., 1996; O'Toole et al., 1996), which have been implicated as modulators of agrin signaling (Hirano and Kidokoro, 1989; Wallace, 1990; Ferns et al., 1993; Mook-Jung and Gordon, 1996; Hopf and Hoch, 1997). In this regard, it is noteworthy that all Z^{+} agrin also contains the Y insert (Ruegg et al., 1992; Hoch et al., 1993). Therefore, Y^{+} and Y^{-} agrin might interact differently with cellular receptors, and the presence of the Y insert might be necessary for Z^{+} agrin to function properly.

Because agrin figures prominently in our current understanding of synaptogenesis, we believed that it was important to obtain more definitive evidence on the roles played by nerve and muscle agrin and by its Y and Z splice variants. Accordingly, we undertook a series of experiments in which we manipulated levels of nerve-derived (Z^{+}), muscle-derived (Z^{-}), and Y^{+} agrin separately. In each case, we assessed the effects of the manipulation on both pre- and postsynaptic differentiation at the NMJ. Our results show that neural Z^{+} agrin alone is required to organize postsynaptic differentiation, that Y^{+} and muscle (Z^{-}) isoforms are dispensable for neuromuscular synaptogenesis, and that agrin is likely to affect presynaptic differentiation indirectly, by way of its effect on the postsynaptic cell.

Results

Roles of Muscle Agrin Studied in Nerve–Muscle Cocultures

We assessed the role of muscle-derived agrin on synapse formation in cocultures of embryonic chick ciliary neurons and myotubes from control or *agrn*$^{neo/neo}$ mice. Myoblasts dissociated from the limb muscles of *agrn*$^{+/neo}$ and *agrn*$^{neo/neo}$ littermates were cultured in rich medium. After myoblasts had fused to form myotubes, neurons dissociated from ciliary ganglia were added to the culture. Ciliary neurons were used in these studies for several reasons: they form cholinergic synapses on striated muscle in vivo yet are far easier to isolate and culture than spinal motoneurons (Bixby and Reichardt, 1985, 1987; Role et al., 1985); their neurites recognize and stop at synaptic sites on skeletal muscle fibers in tissue fragments (Covault et al., 1987); they make Z^{+} agrin and use agrin to organize postsynaptic differentiation in myotubes (Smith and O'Dowd, 1994; Campagna et al., 1997); and they are themselves responsive to recombinant agrin (Campagna et al., 1995; Chang et al., 1997). In both control and mutant cocultures, neurons extended neurites that appeared to run at random and often contacted myotubes. Following 3 days of coculture, differentiation of nerve–muscle contacts was assayed by a triple-labeling protocol: AChRs were labeled with rhodamine-α-bungarotoxin (rBTX), axonal neurofilaments with cascade blue–coupled antibodies to neurofilaments, and synaptic vesicles with fluorescein-coupled antibodies to the intrinsic synaptic vesicle protein SV2.

A well-differentiated nerve–muscle contact from a control culture is shown in Figures 2A–2C. A high-density cluster of AChRs was present on the myotube membrane directly beneath the neurite. The neurite formed a small array of fine branches directly atop the AChR-rich membrane, reminiscent of the terminal arbor seen at NMJs in vivo. The level of SV2—and, by implication, the density of synaptic vesicles—was far higher within these fine terminal branches than in adjoining regions of the same neurite that were not apposed to AChR-rich portions of the myotube. Conversely, levels of neurofilament were higher in the SV2-poor, unbranched portion of the neurite than in the SV2-rich arbor. The concentration of vesicles and paucity of filaments are characteristic of motor nerve terminals in vivo and have been observed at synapses in nerve–muscle cocultures (Lupa et al., 1990).

Approximately 20% of nerve–muscle contacts in control cultures were well-differentiated by criteria shown in Figures 2A–2C (61/298 in six cultures from three animals). Most of the remaining contacts lacked both pre- and postsynaptic differentiation. We do not know why differentiation failed in these cases; neurite and myotube may not have been in close contact (separations of up to several microns would not have been detectable) or contacts may have been newly formed and not yet differentiated. Importantly, however, few contacts showed pre- or postsynaptic differentiation but not both: at only

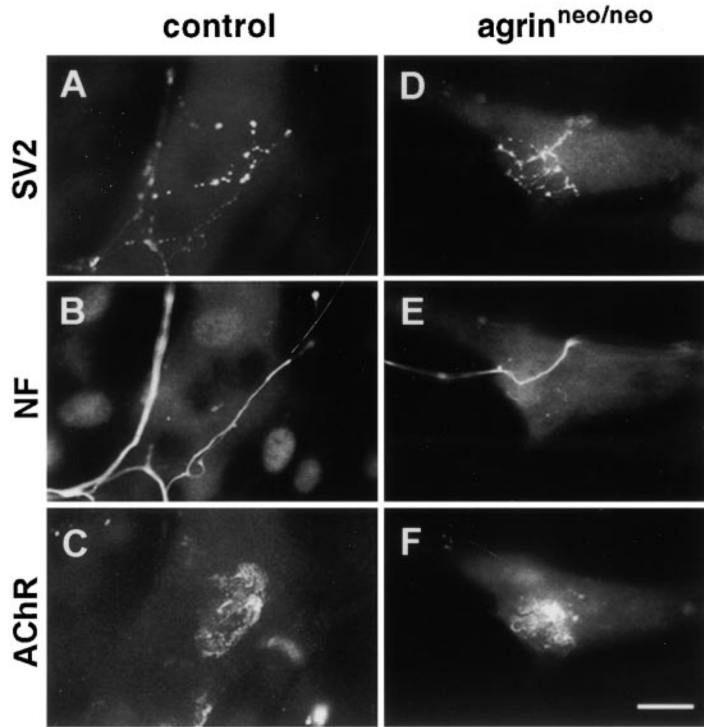

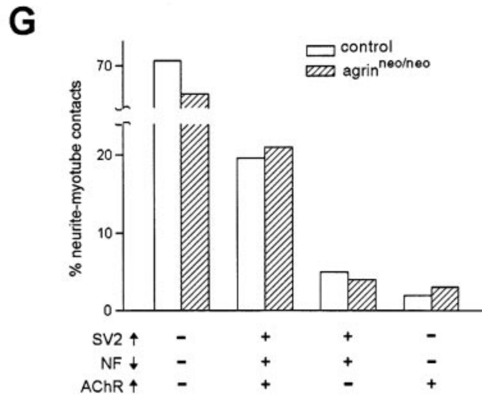

Figure 2. Pre- and Postsynaptic Differentiation at Sites of Nerve–Muscle Contact in Culture

Neurons from embryonic chick ciliary ganglia were added to myotubes prepared from control (A–C) or *agrn*$^{neo/neo}$ neonates (D–F). After 3 days, the cultures were triply stained for the synaptic vesicle protein SV2 (plus fluorescein-conjugated second antibody; [A and D]), neurofilaments (plus Cascade blue–conjugated second antibody; [B and E]), and AChRs (rBTX; [C and F]). AChRs clustered at sites of contact and neurites formed similar SV2-rich, neurofilament-poor presynaptic arbors in control and *agrn*$^{neo/neo}$ myotubes. (G) Shows the percentage of neurite–myotube contacts displaying pre- and/or postsynaptic differentiation. SV2↑, much higher SV2 immunoreactivity in contact area than in adjoining neuritic segment; NF↓, much lower neurofilament immunoreactivity in contact area than in adjoining neuritic segment; and AChR↑, AChR aggregate on myotube precisely opposed to neurite. n = 298 contacts in wild-type cultures and 300 contacts in *agrn*$^{neo/neo}$ cultures. Scale bar, 5 μm (F).

2% of contacts were SV2-poor neuritic segments apposed to an AChR-rich patch of myotube membrane, and at only 5% were SV2-rich varicosities apposed to an AChR-poor patch. Thus, in cocultures as in vivo, pre- and postsynaptic differentiation are coordinated.

Well-differentiated contacts were also observed between ciliary neurites and *agrn*$^{neo/neo}$ myotubes (Figures 2D–2F). No differences in the morphology of contacts or in the incidence of differentiation were detected between cultures prepared from control and *agrn*$^{neo/neo}$ mice (Figure 2G). Thus, lack of muscle-derived agrin does not impair neuromuscular differentiation in vitro.

Roles of Muscle Agrin Studied in Surgical Chimeras

Synaptic contacts remain immature in nerve muscle cocultures, so this system is unsuitable for assessing late stages of synaptic differentiation. To ask whether muscle agrin is required for synaptic maturation, we transplanted sternomastoid muscles from *agrn*$^{+/neo}$ or *agrn*$^{neo/neo}$ neonates into the necks of wild-type adult mice (Figure 3A). The host sternomastoid muscles were denervated and excised, and the remaining nerve stump was affixed to the graft with tissue glue. Immunocompatible hosts were used to avoid the need for immunosuppression, and control transplants were performed with transgene-labeled hosts to rule out the possibility that host-derived myoblasts populated the donor graft (see Experimental Procedures).

Host axons entered wild-type grafts and formed NMJs on donor muscle fibers. By 1 month after transplantation, each muscle fiber in the graft was innervated by a single motor axon terminal arbor rich in synaptic vesicles (synaptophysin-positive; Figure $3D_1$) that abutted an AChR-rich (rBTX-positive; Figure $3D_2$) region of muscle membrane. The overall size of the NMJs in transplanted muscle fibers was smaller compared with normal adult NMJs, probably due to the fact that the grafted muscle

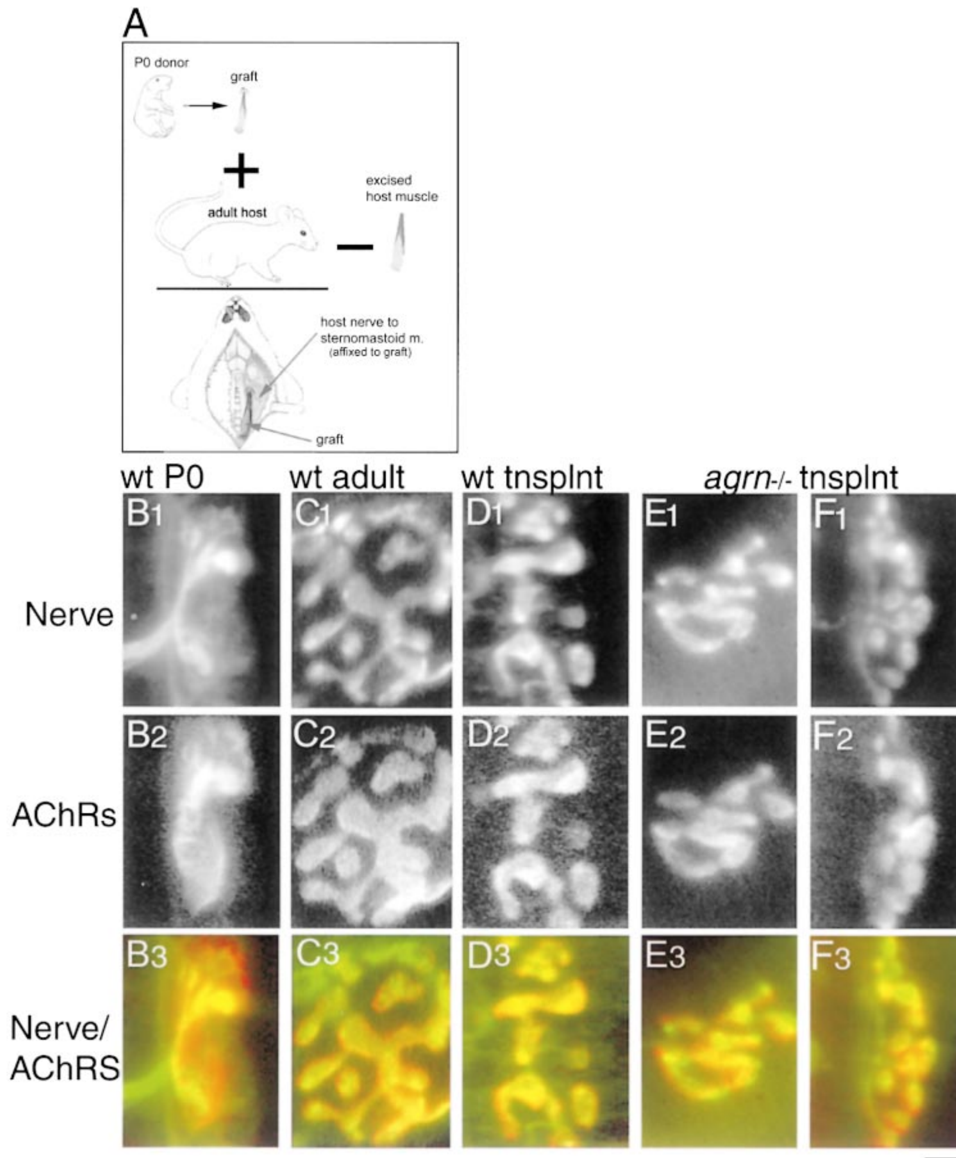

Figure 3. Pre- and Postsynaptic Differentiation at Chimeric NMJs In Vivo

(A) Schematic of transplantation protocol. The left sternomastoid muscle (graft) was excised from a neonate and transferred into the neck of an adult immunocompatible host whose own left sternomastoid muscle had been excised. The host's nerve to the sternomastoid was affixed to the graft to encourage innervation of grafted muscle fibers by host axons. Innervation of the graft by host axons was analyzed 4–6 weeks following transplantation.

(B–F) NMJs from wild-type P0, wild-type adult, wild-type transplanted, and *agrn*$^{neo/neo}$ transplanted muscle fibers.

(B) Wild-type mouse at P0. Nerve terminals (B_1) from multiple axons converge to overlie a muscle membrane region containing a plaque of AChRs (B_2 and B_3).

(C) Wild-type mouse at 6 weeks postnatal. Each muscle fiber receives innervation from a single myelinated axon whose arbors show extensive branching (C_1). The postsynaptic, AChR-rich plaque underlying the presynaptic nerve terminals has formed a highly branched structure (C_2) precisely apposed to the nerve terminals (C_3).

(D) Wild-type graft, 4 weeks following transplantation. The presynaptic (D_1) and postsynaptic (D_2) components of the NMJs in wild-type transplanted muscle fibers exactly oppose each other (D_3). This synapse is singly innervated and shows the branching morphology similar to that seen in normal nontransplanted NMJs.

(E and F) *agrn*$^{neo/neo}$ graft, 6 weeks following transplantation. The morphology of the synapses is indistinguishable from that of wild-type transplants; a single axon (E_1 and F_1) contacting agrin-deficient muscle fibers arborizes over a single high-density branched area of AChRs (E_2 and F_2), and the apposition between the wild-type nerve terminals and postsynaptic AChR clusters is precise (E_3 and F_3). Scale bar, 5 μm (B, D, and F), 8.5 μm (C), and 7.5 μm (E).

fibers did not lengthen at a normal rate and were therefore smaller than their age-matched nontransplanted counterparts. However, the junctions appeared mature in that they consisted of multiple interconnected nerve branches arranged in an ellipse and precisely apposed to AChR-rich gutters (Figure 3D3). The donor graft muscle contracted briskly upon stimulation of the host nerve, indicating that these junctions were functional. In all of

these respects, NMJs formed between host motor axons and wild-type grafted muscle fibers resembled normal adult junctions (Figure 3C). It is important to note that at the time of transplantation, junctions in the graft were immature, with AChRs arranged in a diffuse plaque and each plaque innervated by multiple motor axons (Figure 3B). Thus, synapses made by host motor axons on graft muscle fibers underwent extensive growth and differentiation after grafting and were far more mature than those observed in the nerve–muscle cocultures described above.

Although synaptogenesis was drastically impaired in *agrn*$^{neo/neo}$ muscles in vivo, wild-type motor axons formed elaborate NMJs in *agrn*$^{neo/neo}$ grafts. Each muscle fiber had a single NMJ whose receptor arrangement was indistinguishable from that of control transplants in terms of size and branching complexity (compare Figures $3E_2$ and $3F_2$ with $3D_2$). Neurofilament and synaptophysin staining also showed precise apposition of nerve terminals overlying the postsynaptic AChRs (Figures $3E_1$ and $3F_1$) without extending beyond the boundaries of the postsynaptic membrane (Figures $3E_3$ and $3F_3$). Thus, wild-type motor axons differentiate into mature nerve terminals in the absence of muscle agrin.

In each of three *agrn*$^{neo/neo}$ transplants examined at low power as whole mounts, we observed a well-defined zone of rBTX-positive endplates approximately midway along the length of the grafted muscle (data not shown). This finding was curious in that axons, upon leaving the intramuscular nerve in *agrn*$^{neo/neo}$ neonates, run long distances parallel to the muscle fibers and do not form an end-plate band (Gautam et al., 1996; see below). This result raises the possibility that central regions of myotubes are preferred sites of innervation, but could also reflect preferential growth of wild-type axons through surviving intramuscular nerve sheaths in the graft.

Roles of Z$^+$ Neural Agrin Studied in an Isoform-Specific Mutant

In the previously generated agrin mutant, exons 32 and 33, which encode the Z inserts, were replaced by a selectable marker, *neo*^{r} (Gautam et al., 1996). The resulting mutant, *agrn*$^{neo/neo}$, not only lacked all Z$^+$ agrin but was also a severe hypomorph for all forms of agrin (~90% reduction), presumably because the selectable marker interfered with transcription or transcript stability. To selectively eliminate expression of Z$^+$ agrin, we constructed a modified targeting vector in which the *neo*^{r} gene that replaced exons 32 and 33 was flanked by loxP sites (Figure 4A). Following homologous recombination in embryonic stem (ES) cells, the *neo*^{r} gene was excised with Cre-recombinase (Figure 4B; see Sauer, 1998, for rationale). Analysis of the resulting heterozygous (*agrn*$^{\Delta Z/+}$) and homozygous (*agrn*$^{\Delta Z/\Delta Z}$) mutants indicated that the Z exons had been deleted and the *neo*^{r} gene excised (Figure 4C).

We used PCR and immunohistochemistry to assess expression of agrin in the *agrn*$^{\Delta Z/\Delta Z}$ mutant. First, agrin transcripts were analyzed by RT-PCR with primers complementary to exons 31 and 34, which flank the Z exons (Figure 4D). Bands corresponding to the Z$^+$ isoforms were amplified from control but not *agrn*$^{\Delta Z/\Delta Z}$ tissue, confirming the deletion of the Z exons. In contrast, the band derived from Z$^-$ agrin RNA was present in both samples. The absence of the Z$^+$ exons and the presence of common exons were confirmed by hybridization of the PCR products with exon-specific probes (Figure 4E). Using similar methods, we assayed expression of the Y exon in the mutant. Most transcripts from *agrn*$^{\Delta Z/\Delta Z}$ and control CNS tissue contained the Y exon, whereas most transcripts from *agrn*$^{\Delta Z/\Delta Z}$ and control muscles lacked this transcript (Figure 4F). Thus, even though all Z$^+$ agrin is also Y$^+$ in normal animals (Ruegg et al., 1992; Hoch et al., 1993), deletion of Z exons does not prevent inclusion of the Y exon. Moreover, the normal preponderance of Y$^+$ agrin in central nervous tissue and of Y$^-$ agrin in muscle is unchanged in the *agrn*$^{\Delta Z/\Delta Z}$ mutant.

Finally, we stained muscles from neonatal mutants and controls with an antiserum that recognizes all agrin isoforms (Figure 4G). At this stage, agrin was present throughout the muscle fiber basal lamina in control and *agrn*$^{\Delta Z/\Delta Z}$ but was barely detectable in *agrn*$^{neo/neo}$ muscle. To further document the retention of muscle agrin in the *agrn*$^{\Delta Z/\Delta Z}$ mutant, we performed quantitative immunofluorescence measurements on embryonic day 18 (E18) myotubes stained with anti-agrin. Levels of extrasynaptic muscle agrin did not differ significantly between control and *agrn*$^{\Delta Z/\Delta Z}$ mice ($n = 24$ fibers from four sections for each genotype), whereas levels in *agrn*$^{neo/neo}$ mice were only 12% of those in *agrn*$^{\Delta Z/\Delta Z}$ ($n = 24$). Likewise, levels of agrin were apparently normal in the kidney, lung, and cerebral vasculature of *agrn*$^{\Delta Z/\Delta Z}$ mice (data not shown). Thus, whereas replacement of the Z exons with a selectable marker leads to decreased levels of all agrin isoforms (Gautam et al., 1996), subsequent removal of the selectable marker permits expression of Z$^-$ isoforms and thereby leads to selective loss of Z$^+$ splice variants.

agrn$^{\Delta Z/\Delta Z}$ mice were stillborn or died immediately after birth, did not inflate their lungs, and were never seen to move spontaneously. In controls, motor axons enter muscles such as the diaphragm and form an intramuscular nerve. Individual axons then leave the nerve and branch; each branch contacts a myotube, arborizes, and induces formation of an AChR-rich postsynaptic apparatus. Each myotube bears a single, AChR-rich endplate, and most endplates are located in a central band near the intramuscular nerve (Figures 5A and 5B). In *agrn*$^{\Delta Z/\Delta Z}$ mice, an intramuscular nerve formed, and axons left the nerve (Figures 5C and 5D). However, the axons failed to stop and arborize but instead ran long distances parallel to myotubes. AChR clusters were fewer in number, ~30% smaller in size, and significantly lower in density (rBTX staining intensity) than clusters in control muscle. Most axons ended on AChR-poor regions of myotube membrane, at least two-thirds of AChR clusters were not opposed by neurites (Figures 5E and 5F), and many clusters were outside of the central end-plate band. All synaptic antigens tested, including basal laminae components such as acetylcholinesterase and cytoskeletal elements such as rapsyn, codistributed with AChRs at both neural and aneural AChR clusters (data not shown). In all of these respects, *agrn*$^{\Delta Z/\Delta Z}$ mice were indistinguishable from the *agrn*$^{neo/neo}$ mice described previously (Gautam et al., 1996). Thus, both pre- and postsynaptic differentiation were severely impaired in the absence of Z$^+$ agrin, despite the presence of near normal levels of Z$^-$ agrin.

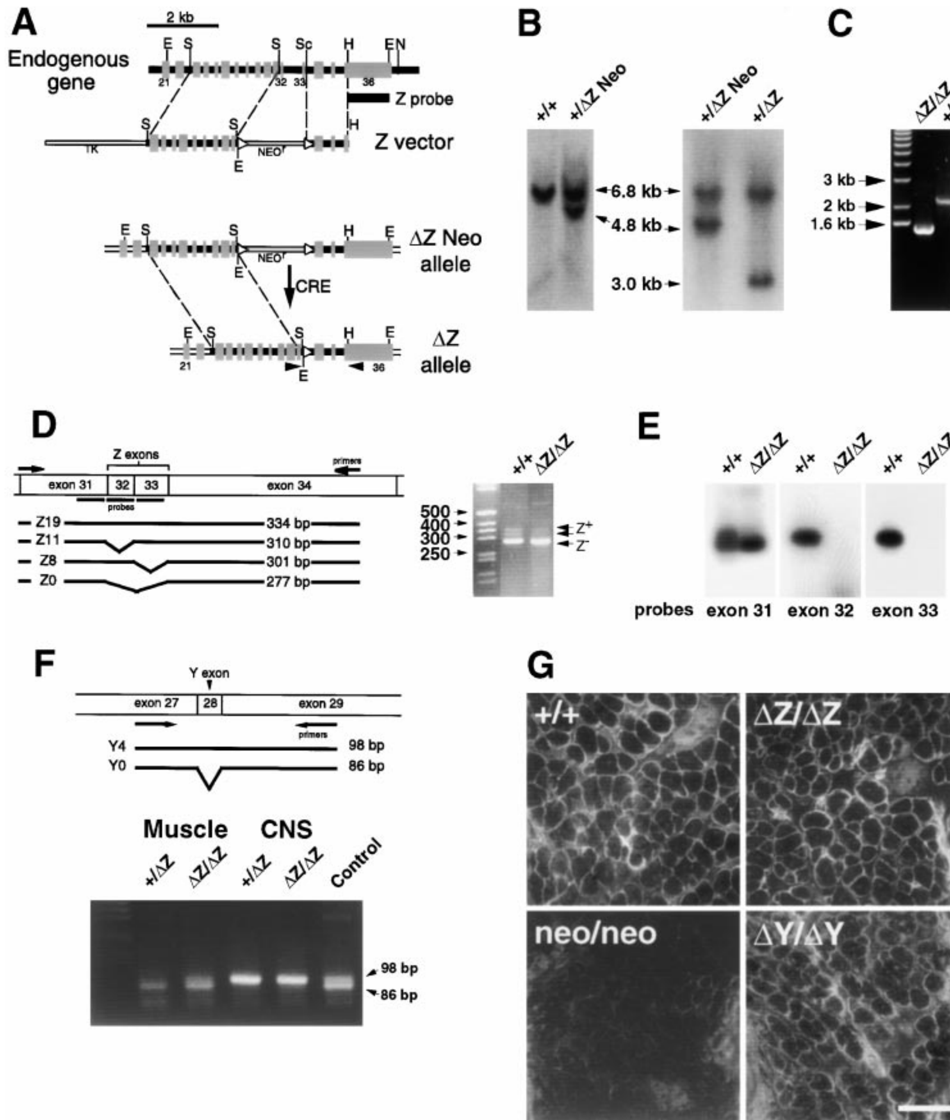

Figure 4. Generation of a Z-Specific Agrin Mutant

(A) In the targeting vector, a selectable marker (*neo*^{r}) flanked by loxP sites replaced the Z exons. Homologous recombination followed by Cre-mediated excision of the selectable marker deleted the Z exons. Probe used for Southern analysis in (B) and primers used for genotyping in (C) are indicated (E, EcoRI; H, HindIII; N, NotI; S, SphI; and Sc, ScaI).

(B) Southern analysis of EcoRI-digested genomic DNA from control ES cells, a homologous recombinant clone, and a Cre-transfected subclone.

(C) PCR analysis of DNA from *agrn*$^{+/+}$ and *agrn*$^{\Delta Z/\Delta Z}$ mice.

(D) RT-PCR analysis of RNA from brains of *agrn*$^{+/+}$ and *agrn*$^{\Delta Z/\Delta Z}$ mice using primers that flanked the Z exons. Bands corresponding to Z^+ isoforms are absent from the mutant. Diagram shows position of primers, size of expected products, and probes used in (E).

(E) Southern analysis of PCR products shown in (D) using exon-specific probes. Z exon–containing RNA was present only in controls, but mRNA containing flanking exons was present at similar levels in controls and mutants.

(F) RT-PCR analysis of Y^- and Y^+ RNA from CNS (brains and spinal cord) and muscle of control and *agrn*$^{\Delta Z/\Delta Z}$ mice using primers that flanked the Y exon. Bands corresponding to Y^+ isoforms are more abundant in CNS than in muscle in both *agrn*$^{+/\Delta Z}$ and *agrn*$^{\Delta Z/\Delta Z}$. Control lane is from a whole control E18 embryo. Diagram shows position of primers and size of expected products.

(G) Sections of intercostal muscle from control, *agrn*$^{neo/neo}$, *agrn*$^{\Delta Z/\Delta Z}$, and *agrn*$^{\Delta Y/\Delta Y}$ neonates stained with an antiserum that recognizes all isoforms of agrin. Scale bar, 50 μm.

Roles of Y^+ Agrin Studied in an Isoform-Specific Mutant

Using the strategy described above for the *agrn*$^{\Delta Z}$ allele, we generated a mutant in which expression of Y^+ agrin was selectively eliminated. As shown in Figure 6A, in exon 28, the Y exon was replaced with a *neo*^{r} gene flanked by loxP sites. Southern analysis and PCR of genomic DNA confirmed deletion of exon 28 and Cre-mediated excision of the *neo*^{r} gene (Figures 6B and 6C). RT-PCR analysis showed that transcripts from the resulting *agrn*$^{\Delta Y/\Delta Y}$ mutants lacked the Y exon. Whereas most agrin RNA in the CNS of wild-type mice was Y^+, Y^- transcripts were abundant in mutants (Figure 6D), indicating that agrin RNA was transcribed and stable.

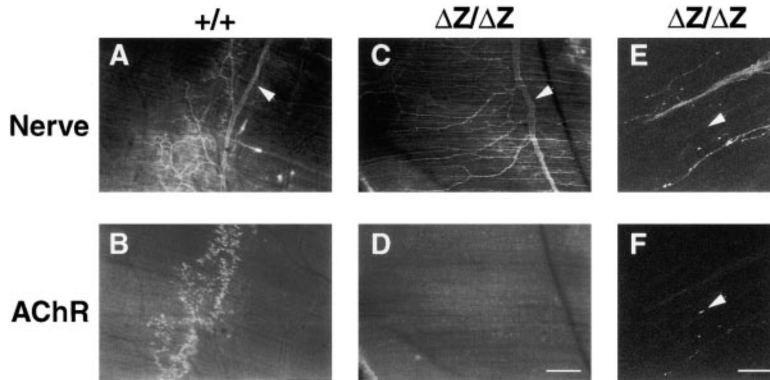

Figure 5. Impaired Synaptic Differentiation in the Absence of Z^+ Agrin

(A–D) Diaphragm muscles from E18 control (A and B) and *agrn*$^{\Delta Z/\Delta Z}$ neonates, double stained with antibodies to neural antigens (A and C) and rBTX (B and D). In controls, axons leave the intramuscular nerve (arrowhead) and terminate at AChR-rich patches of myotube membrane. In mutants, AChR-rich patches are small and usually uninnervated, and axons run long distances parallel to the myotube.

(E and F) Higher magnification micrograph of an axon and an AChR-rich patch in an *agrn*$^{\Delta Z/\Delta Z}$ muscle, showing lack of correspondence between pre- and postsynaptic elements. Arrowheads mark site of an aneural AChR cluster. Scale bar, 200 μm (D) and 25 μm (F).

Expression and splicing of the Z exons was apparently unaffected by deletion of Y (Figure 6E), despite their normally coordinate expression (Hoch et al., 1993).

Immunohistochemical studies showed that the distribution of agrin in *agrn*$^{\Delta Y/\Delta Y}$ muscle and kidney did not differ detectably from that in controls, and quantitative immunofluorescence measurements of anti-agrin stained-sections showed that levels of agrin did not differ significantly between *agrn*$^{+/+}$ and *agrn*$^{\Delta Y/\Delta Y}$ tissues (Figures 4G, 7B, and 7D; data not shown).

agrn$^{\Delta Y/\Delta Y}$ mutants were viable, active, fertile, and externally normal. In mutants, as in control NMJs, differentiated nerve terminals directly apposed an AChR-rich postsynaptic membrane, and extensive histological analysis revealed no abnormalities either during early postnatal maturation or in adulthood (data not shown). We therefore performed additional studies designed to reveal subtle roles of Y^+ agrin. First, we analyzed NMJs in 8-month-old *agrn*$^{\Delta Y/\Delta Y}$ mice to test the possibility that the Y exon or its ability to bind heparin is necessary for long-term maintenance of the synapse. However, agrin remained concentrated at synapses in mutants, and synaptic structure remained normal (Figures 7A–7D). Second, we attempted to destabilize the postsynaptic membrane by denervation to test the possibility that the Y exon or its heparin-binding ability is necessary for maintenance of postsynaptic specializations in the absence of the nerve. However, agrin remained concentrated in synaptic basal lamina, and AChRs remained concentrated in the postsynaptic membrane for up to 9 days after denervation (Figures 7E and 7F). Third, we assessed the reinnervation of muscle following nerve

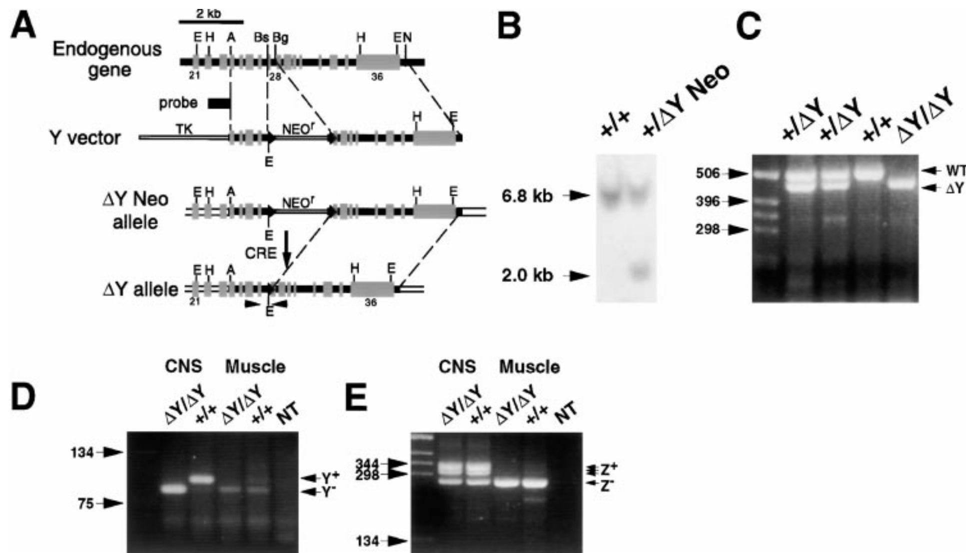

Figure 6. Generation of a Y-Specific Agrin Mutant

(A) In the targeting vector, a selectable marker (*neo^r*) flanked by loxP sites replaced the Y exon. Homologous recombination followed by Cre-mediated excision of the selectable marker deleted the Y exon. Probe used for Southern analysis in (B) and primers used for genotyping in (C) are indicated (A, AflIII; E, EcoRI; Bs, Bsp106; Bg, BglI; and H, HindIII).

(B) Southern analysis of EcoRI-digested genomic DNA from control ES cells and a homologous recombinant clone.

(C) PCR analysis of *agrn*$^{+/+}$, *agrn*$^{+/\Delta Y}$, and *agrn*$^{\Delta Y/\Delta Y}$ mice following Cre excision of the *neo^r* cassette.

(D and E) RT-PCR analysis of RNA from brains of 2-day-old *agrn*$^{+/+}$ and *agrn*$^{\Delta Y/\Delta Y}$ mice using primers that flanked the Y and Z exons. A band corresponding to the Y isoform is present only in the control (D), whereas Z^+ isoforms are present in both mutant and control (E). See Figure 4 for positions of primers and sizes of expected products.

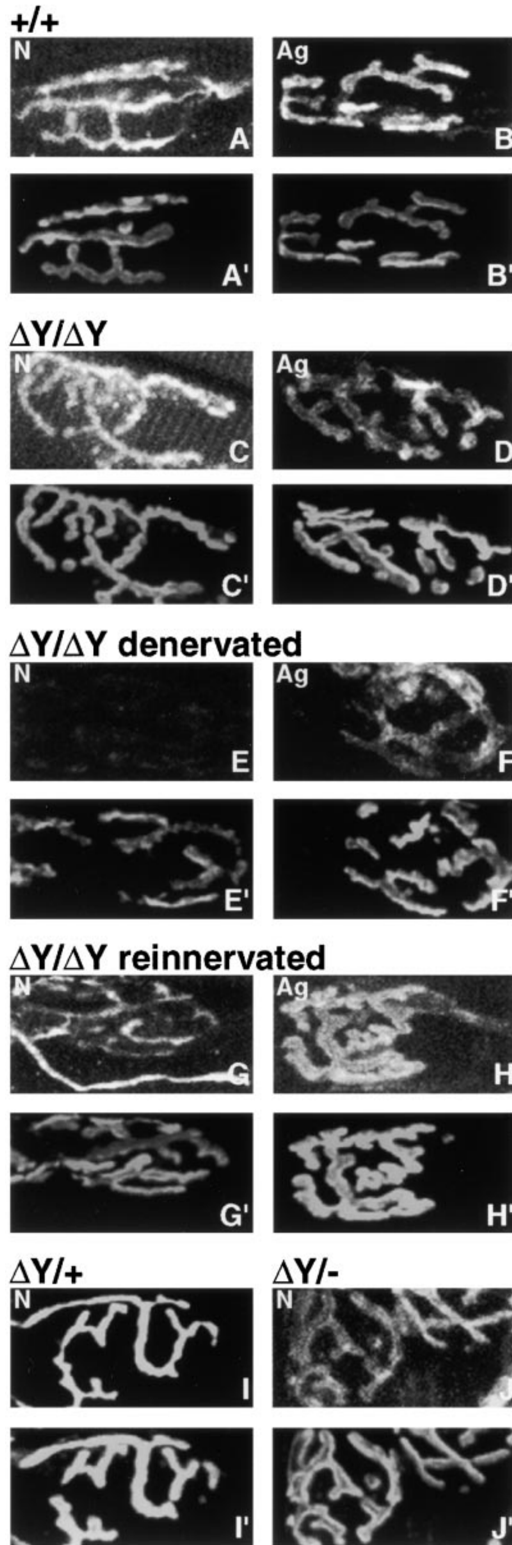

Figure 7. Neuromuscular Differentiation in the Absence of Y^+ Agrin

Longitudinal sections were doubly stained with antibodies to neural antigens (A, C, E, G, I, and J) plus rBTX (A′–J′).

(A and B) Wild type (8-month-old).

(C and D) *agrn*$^{\Delta Y/\Delta Y}$ (8-month-old).

(E and F) *agrn*$^{\Delta Y/\Delta Y}$ (8-month-old) denervated by cutting the motor nerve 9 days before sacrifice.

(G and H) *agrn*$^{\Delta Y/\Delta Y}$ (8-month-old) subjected to denervation and reinnervation by nerve crush 14 days before sacrifice.

(I) Control (3-month-old).

(J) *agrn*$^{\Delta Y/-}$ (2-month-old). In all cases, the structure of the synapse and the synaptic concentration of agrin were indistinguishable in controls and mutants.

damage to test the possibility that the Y exon is essential for synaptic regeneration rather than development. However, reinnervation proceeded on schedule and normally in the absence of Y^+ agrin (Figures 7G and 7H). Finally, to reduce the dosage of agrin, we crossed *agrn*$^{\Delta Y/\Delta Y}$ mice to mice lacking all forms of agrin and analyzed the transheterozygous offspring. Again, no abnormalities were found (Figures 7I and 7J).

Discussion

We have used nerve–muscle cocultures, surgical chimeras, and two new agrin mutant alleles to assess the roles of several agrin isoforms and sources in the formation of the NMJ. We found that synaptic development is severely impaired in the absence of Z^+ agrin, which is made by motoneurons but not by myotubes and Schwann cells. In contrast, apparently normal synapses form in the absence of muscle agrin. Taken together, these results provide strong genetic evidence for the hypothesis (McMahan, 1990) that agrin is a critical, nerve-derived organizer of synaptic differentiation. In addition, our results led to two less predictable conclusions. First, Z^-, Y^+, and muscle-derived pools of agrin are dispensable for major steps in synaptic differentiation. Second, agrin promotes presynaptic differentiation by causing the postsynaptic apparatus to produce or localize retrograde signals other than agrin itself.

Y^+, Z^-, and Muscle Agrins

Although most attention has focused on the AChR-clustering ability of Z^+ agrin, Z^- isoforms have been shown to have several activities. Z^- agrin can induce AChR clustering in some assays (Campanelli et al., 1991; Ferns et al., 1992), modulate Z^+ agrin–stimulated phosphorylation of AChRs (Meier et al., 1998b), stimulate AChR gene expression (Jones et al., 1996; Meier et al., 1998a), serve as a stop signal for neurites, and induce some elements of presynaptic differentiation (Campagna et al., 1995, 1997; Chang et al., 1997). Z^- agrin also binds to numerous putative agrin receptors on the myotube surface, including neural cell adhesion molecule, α-dystroglycan, pleiotrophin, laminin, and integrins (Biroc et al., 1993; Hoch et al., 1994; Sugiyama et al., 1994; Burg et al., 1995; Campanelli et al., 1996; Gesemann et al., 1996; Denzer et al., 1997; Martin and Sanes, 1997). Most of these receptors bind both Z^- and Z^+ agrin equally well, and α-dystroglycan binds more avidly to Z^- than to Z^+ agrin. Both Z^- and Z^+ agrin bear follistatin-like domains that can bind growth factors and serve as protease inhibitors. Finally, the Y insert endows agrin with the ability to bind heparin, which seemed likely to modulate agrin's interactions with membrane- and matrix-associated heparan sulfate proteoglycans (Campanelli et al., 1996; Gesemann et al., 1996; O'Toole et al., 1996; Hopf and Hoch, 1997).

We used four strategies to assess the functions of Z^- agrin isoforms. First, we compared synaptic differentiation at contacts made by wild-type neurons on control and agrin-deficient myotubes. No differences were observed. Second, we studied the formation of NMJs between wild-type motoneurons and agrin-deficient muscle fibers in surgical chimeras. This approach circumvented the neonatal lethality of the *agrn*$^{neo/neo}$ mutant and permitted us to analyze late steps in synaptic maturation. However, we found no abnormalities in the chimeric synapses. Third, we compared the phenotype of the *agrn*$^{neo/neo}$ mutant, deficient in all forms of agrin, with that of the *agrn*$^{\Delta Z/\Delta Z}$ mutant, which lacked only Z^+ agrin. We reasoned that differences between the phenotypes of the two alleles would reveal roles of Z^- agrin. However, no differences were seen. Finally, we generated mutants that lacked Y agrin. In these mutants, agrin was presumably unable to bind to heparan sulfate side chains on proteoglycans. However, levels of agrin in basal laminae were reduced only slightly if at all relative to controls, and NMJs appeared normal both during development and in adults.

One limitation of this analysis is that the original agrin mutant, *agrn*$^{neo/neo}$, is a hypomorph rather than a null; it lacks Z^+ agrin completely but produces low levels of Z^- agrin. Our analysis suggests that agrin levels in this mutant are 10%–15% of those in controls. Therefore, the possibility must be considered that the low levels of muscle-derived Z^- agrin in nerve–muscle cocultures or surgical chimeras are required for synaptic differentiation. Although we cannot completely exclude this possibility, we believe it to be unlikely; although some agrin is present in mutant muscle in vivo (Figure 4G), no agrin is detectable on the surface of myotubes cultured from *agrn*$^{neo/neo}$ mutants (Gautam et al., 1996).

Our results do not imply that Z^- agrin plays no role in vivo. Agrin is abundant in the CNS (O'Connor et al., 1994; Stone and Nikolics, 1995; Cohen et al., 1997b; Li et al., 1997) and has been hypothesized to play a role in central axon outgrowth, synaptogenesis, or plasticity (McMahan et al., 1992; Bowe and Fallon, 1995; Halfter et al., 1997). Initial studies of hippocampal neurons cultred from *agrn*$^{neo/neo}$ mice have failed to substantiate this idea (Serpinskaya et al., 1999), but the neonatal lethality of the mutant has prevented study of agrin's role in the maturation, stability, or plasticity of central synapses in vivo. Likewise, we have so far been unable to address the possibility that Z^- agrin plays a role in postnatal development or in the function of nonmuscle tissues such as lung and kidney, in which it is abundantly expressed. Finally, no agrin homologs have been identified to date, but distantly related proteins such as perlecan or laminin may compensate for loss of agrin.

Agrin and Presynaptic Differentiation

Motor axons form few arbors and differentiate poorly in *agrn*$^{neo/neo}$ mutants. As noted in the Introduction, these defects could reflect direct actions of agrin on nerves and/or be secondary consequences of impaired postsynaptic differentiation. In favor of a direct mechanism, three groups have now shown that both Z^- and Z^+ agrin have clear effects on cultured neurons: they are adhesive for spinal motoneurons, ciliary motoneurons, sensory neurons, and retinal neurons; they inhibit neurite outgrowth from all four neuronal types; and they promote the aggregation of synaptic vesicles in ciliary motoneurons (Burg et al., 1995; Campagna et al., 1995, 1997; Chang et al., 1997; Halfter et al., 1997). It is therefore plausible that nerve-derived Z^+ agrin promotes postsynaptic differentiation, whereas muscle-derived Z^- agrin promotes presynaptic differentiation.

Our results do not support this possibility. Motor axons innervating agrin-deficient myotubes in cultures and in surgical chimeras differentiate normally, indicating that muscle agrin is not necessary for presynaptic differentiation. Conversely, motor axons innervating *agrn*$^{\Delta Z/\Delta Z}$ myotubes, which are rich in Z^- agrin, fail to differentiate, indicating that muscle agrin is not sufficient for presynaptic differentiation. Thus, either presynaptic differentiation is selectively induced by Z^+ agrin, or the effects of agrin on neurites are secondary to Z^+ agrin–dependent postsynaptic differentiation. In that Z^+ and Z^- agrin are equally adhesive for neurons and equally potent in inhibiting neurite outgrowth and promoting vesicle clustering (Campagna et al., 1997; Chang et al., 1997; D. Dickman et al., unpublished data), we favor the second alternative. Further support for this idea comes from mutant mice lacking muscle-specific kinase (MuSK), the leading candidate agrin receptor (DeChiara et al., 1996). These mice exhibit both pre- and postsynaptic defects similar to those in *agrn*$^{neo/neo}$ mice even though MuSK is not expressed by neurons (Valenzuela et al., 1995), and agrin is present on the surface of *MuSK*$^{-/-}$ muscle (M. Gautam et al., submitted).

Our results in vitro contrast with those of Campagna et al. (1997). These workers cultured ciliary motoneurons with chick myotubes and assayed pre- and postsynaptic differentiation immunohistochemically, as we did. They showed that high concentrations (200 μg/ml) of anti-agrin IgG blocked both pre- and postsynaptic differentiation, whereas a lower concentration (100 μg/ml) exerted a selective effect on presynaptic differentiation. They suggested that the lower dose of antiserum selectively affected a site on agrin with which neurites interact and concluded that agrin directly affects presynaptic differentiation. However, even though the lower dose of antiserum failed to block postsynaptic differentiation completely, it did have significant effects on the size and shape of nerve-induced AChR clusters. In light of our results, it seems possible that the presynaptic effect Campagna et al. (1997) observed was in fact a consequence of perturbed postsynaptic differentiation.

If agrin is not the primary organizer of presynaptic differentiation, what is? Candidates include laminin subunits such as β2, which are concentrated, along with agrin, in synaptic basal lamina. Laminin β2 can induce motor axons to stop growing and begin differentiating into nerve terminals in vitro (Porter et al., 1995; Patton et al., 1997), and presynaptic differentiation is impaired in *laminin β2* mutants (Noakes et al., 1995). On the other hand, the presynaptic defects in *laminin β2* mutants are far milder than those in *agrin* and *MuSK* mutants, indicating that additional and perhaps earlier acting retrograde signals exist. Several candidates have been proposed, based on their activities in vitro (Dai and Peng, 1996). It will be important to assess their roles in vivo.

Experimental Procedures

Nerve–Muscle Cocultures

Methods for preparing nerve–muscle cocultures were modified from Lupa et al. (1990). Briefly, mononucleated cells were dissociated from hindlimbs of E18 embryos and plated on collagen-coated wells of a multichamber slide (Nunc). The culture medium was Dulbecco's modified Eagle's medium (DMEM) containing 5% fetal calf serum, 10% horse serum, and 3% chick embryo extract. Three days after plating, 10 μM cytosine arabinoside was added to suppress proliferation of undifferentiated cells. One day later, the medium was replaced by DMEM containing 5% horse serum and 3% chick embryo extract but no calf serum or cytosine arabanoside. Two days later, after myotubes had formed, neurons were dissociated from E10–E12 chick ciliary ganglia and plated on the myotubes. At this time, 1.5% chick eye extract was added to the medium. Three days later, rBTX was added for 1 hr to label AChRs, and the cultures were then fixed in 1% paraformaldehyde in phosphate-buffered saline (PBS). Fixed cultures were stained with mouse anti-SV2 antibody and rabbit anti-neurofilament (Sigma), followed by fluorescein-conjugated goat anti-mouse IgG (Cappel, Durham, NC) and Cascade blue–conjugated goat anti-rabbit IgG (Molecular Probes, Eugene, OR).

Surgical Chimeras

Methods for transplantation are detailed elsewhere (Q. T. N. et al., unpublished data). Briefly, adult mice were anesthetized with ketamine and xylazine, a ventral midline incision was made in the neck, and the left sternomastoid muscle was removed, leaving a long portion of the nerve to the sternomastoid intact. P0 mouse pups (*agrn*$^{neo/neo}$ mutants or littermate controls) were anesthetized with ice, perfused transcardially with DMEM, and then immersed completely in DMEM. The left sternomastoid and cleidomastoid muscles (henceforth referred to as graft) were rapidly dissected with their bony insertions intact and immediately transferred into the neck of the host animal. The distal insertion of the graft was attached to the sternum of the host with two 9–0 monofilament sutures (Ethicon). The proximal insertion of the graft was sutured by affixing the mastoid process of the temporal bone of the donor tissue to the host animal's left digastric muscle with one suture. The host nerve stump to the sternomastoid muscle was attached to the mastoid process of the temporal bone of the graft with tissue glue (Nexaband, Veterinary Products Laboratories). The wound was then sutured closed and the host animal returned to its cage for recovery. Innervation of grafts by host axons was analyzed by staining with rBTX for AChRs and with antibodies to neurofilament and synaptophysin (see above) 2 weeks to 6 months following transplantation.

Three strains of mice were used as hosts for wild-type, mutant, and control transplants. F1 offspring of C57BL6 and 129SvJ parents were used for *agrn*$^{neo/neo}$ and control transplants. The mutants were generated from 129JES cells and maintained on a mixed C57BL6–129 background, so use of F1 hosts ensured immunocompability and thus obviated the need for immunosuppression following transplantation. ROSA-26, which express cytoplasmic β-galactosidase in their muscles (obtained from Jackson Laboratories) and RNZ mice, which express nuclear localized β-galactosidase in their muscles (Pin et al., 1997), were used as control hosts for wild-type grafts. In these controls, we asked whether any muscle fibers in the graft incorporated host-derived myoblasts, but found none. These controls are presented in Q. T. N. et al. (unpublished data).

Generation of *agrn*$^{\Delta Y}$ and *agrn*$^{\Delta Z}$ Mutants

The *agrn*$^{\Delta Z}$ targeting vector was constructed in the ploxPneo-1 vector, a generous gift of A. Nagy (Toronto, Ontario, Canada). In this vector, a lox–*neo*^{r}–lox cassette replaced a 700 bp fragment of the *agrn* gene that included exons 32 and 33 as well as 92 bp of the 169 bp intron 31 and 14 bp of the 266 bp intron 33 (Rupp et al., 1992). The 5′ region of homology was a 3.5 kb SphI fragment (Gautam et al., 1996) that extended from intron 22 to intron 31. The 3′ homology region was a 1.1 kb SacI–HndIII fragment that extended from intron 33 to exon 36. The thymidine kinase gene was removed from the pPNT vector by EcoRI–HindIII digestion and blunted with Klenow. This was then cloned into the NruI site of pSL1180, removed with SacII and NotI, and recloned into the SacII–NotI sites of the ploxPneo-1 multiple cloning site.

Mutant mice were generated by electroporating RI ES cells (Nagy et al., 1993) with linearized vector and selecting with 250 μM G418 and 2.7 μM FIAU for 9–11 days. Colonies were screened by Southern blotting for homologous recombinations, following digestion of genomic DNA with EcoRI. The wild-type EcoRI fragment is 6.8 kb but is reduced to 4.8 kb in homologous recombinants because of the two EcoRI sites in the ploxPneo-1 vector (Figure 3A). Cells from two recombinant clones were transiently transfected with a Cre expression plasmid (provided by A. Nagy, University of Toronto) and plated at clonal density without antibiotic selection. Individual clones were picked and screened by PCR and Southern blotting for the removal of the *neo*^{r} gene. For each of the original recombinant clones, ∼10% of the transiently transfected clones were completely lacking the *neo*^{r} gene. One *neo*^{r} excised line was expanded and injected into C57BL6 blastocysts, which were implanted into ICR pseudopregnant females.

The *agrn*$^{\Delta Y}$ targeting vector was constructed from ploxPneo-1 and the thymidine kinase gene as described above. In this vector, the lox–*neo*^{r}–lox cassette replaced a 150 bp fragment of the *agrn* gene that included exon 28, 7 bp of the 209 bp intron 27, and 160 bp of the 210 bp intron 28. The 5′ region of homology consisted of a 1.1 kb AflIII–Bsp106 fragment that extended from intron 23 to intron 27. The 3′ region of homology was a 5 kb BglI–NotI fragment that extended from intron 28 to ∼500 bp downstream of the final exon (exon 36). ES cells were transfected and screened as above, except an 800 bp HindIII–AflIII probe was used for Southern analysis. Five recombinant lines were isolated from ∼200 colonies screened, and germline transmission of the *agrn*$^{\Delta Y}$ allele was achieved with two independent clones. The *neo*^{r} gene was excised from the genome in vivo by mating to transgenic mice that express Cre under the control of regulatory elements from the β-*actin* gene (kind gift of Mark Lewandoski, University of California, San Francisco; Lewandoski and Martin, 1997).

The *agrn*$^{\Delta Z/\Delta Z}$ allele differed from the original *agrn*$^{neo/neo}$ allele in that *agrn*$^{\Delta Z}$ lacked the *neo*^{r} cassette, which was retained in the *agrn*$^{neo/neo}$ mutant. All forms of agrin were depleted when the *neo*^{r} gene was retained, whereas its excision with Cre-recombinase generated an allele in which Z^+ agrin was selectively affected. Likewise, we found that all forms of agrin were depleted in mice bearing the *agrn*$^{\Delta Y/\Delta Y}$ allele in which the *neo*^{r} gene was retained (data not shown), whereas Y^+ agrin was selectively affected following excision of *neor* with Cre-recombinase. Thus, in both cases, insertion of *neo*^{r} into the *agrin* gene exerts a dramatic and general effect on transcription or transcript stability.

Transcript Analysis

Tissues were homogenized in guanidinium isothiocyanate using a Polytron, and total RNA was prepared (Chomczynski and Sacchi, 1987). Aliquots of RNA (10 μg) were then reverse transcribed with avian myeloblastosis virus reverse transcriptase with a mix of oligo dT and random primers. This first strand cDNA was then used as the template for PCR. Reaction products were separated on 2%–4% agarose gels. In some cases, the products were then denatured and blotted onto GeneScreen Plus membranes, and the blots were probed with ^{32}P-labeled oligonucleotides.

Histological Methods

Muscles were frozen, sectioned in a cryostat, and immunostained as described previously. Cross sections of unfixed tissue were cut at 8–10 μm and fixed in cold methanol before staining. Longitudinal sections of paraformaldehyde-fixed tissue were cut at 40 μm. Antibodies included mouse anti-SV2 (a generous gift of K. Buckley, Harvard), rabbit anti-AChE, mouse anti-rapsyn, rabbit anti-agrin (provided by Regeneron Pharmaceuticals), mouse anti-NF200 (SM321, Sternberger Monoclonals), rabbit anti-synaptophysin (G95), rabbit anti-NF200 (Sigma), FITC-conjugated anti-mouse IgG1 (Boehringer Mannheim), Cy3-conjugated goat anti-rabbit IgG (Molecular Probes), and FITC-conjugated goat anti-rabbit IgG (Cappel). Texas red- or tetramethylrhodamine B isothiocyanate–conjugated α-bungarotoxin (Molecular Probes) was included with the secondary antibody. For quantitative immunofluorescence measurements, images

were captured with a cooled charge-coupled device camera and processed with IPLab software (Signal Analytics, Vienna, VA).

For analysis of whole mounts, muscles were fixed for 15 min in 2% paraformaldehyde in PBS and washed in 0.1 M glycine in PBS for >2 hr. The muscles were then incubated successively for 8–18 hr in each of the following solutions: (1) PBS containing 2 mg/ml bovine serum albumin and 1% Triton X-100 (PBSBT), (2) primary antibodies (usually anti-NF200 plus anti-synaptophysin) in PBSBT, (3) PBSBT, (4) secondary antibodies (usually FITC goat anti-rabbit IgG) plus Texas red α-bungarotoxin in PBSBT, and (5) PBSBT. Finally, the muscles were mounted between coverslips in glycerol plus paraphenylenediamine. Data presented are representative of >20 control, 12 $agrn^{\Delta Z/\Delta Z}$, and 15 $agrn^{\Delta Z/\Delta Z}$ mice examined.

Acknowledgments

We thank Carol Borgmeyer, Jimmy Gross, Mia Nichol, and Sherry Weng for help with the mice and Fabio Rupp and Richard Scheller for genomic clones. This work was supported by grants from the National Institutes of Health.

Received December 30, 1998; revised March 23, 1999.

References

Biroc, S.L., Payan, D.G., and Fisher, J.M. (1993). Isoforms of agrin are widely expressed in the developing rat and may function as protease inhibitors. Dev. Brain Res. *75*, 119–129.

Bixby, J.L., and Reichardt, L.F. (1985). The expression and localization of synaptic vesicle antigens at neuromuscular junctions *in vitro*. J. Neurosci. *11*, 3070–3080.

Bixby, J.L., and Reichardt, L.F. (1987). Effects of antibodies to neural cell adhesion molecule (N-CAM) on the differentiation of neuromuscular contacts between ciliary ganglion neurons and myotubes *in vitro*. Dev. Biol. *119*, 363–372.

Bowe, M.A., and Fallon, J.R. (1995). The role of agrin in synapse formation. Annu. Rev. Neurosci. *18*, 443–462.

Burg, M.A., Halfter, W., and Cole, G.J. (1995). Analysis of proteoglycan expression in developing chicken brain: characterization of a heparan sulfate proteoglycan that interacts with the neural cell adhesion molecule. J. Neurosci. Res. *41*, 49–64.

Campagna, J.A., Ruegg, M.A., and Bixby, J.L. (1995). Agrin is a differentiation-inducing "stop signal" for motoneurons in vitro. Neuron *15*, 1365–1374.

Campagna, J.A., Ruegg, M.A., and Bixby, J.L. (1997). Evidence that agrin directly influences presynaptic differentiation at neuromuscular junctions in vitro. Eur. J. Neurosci. *9*, 2269–2283.

Campanelli, J.T., Hoch, W., Rupp, F., Kreiner, T., and Scheller, R.H. (1991). Agrin mediates cell contact–induced acetylcholine receptor clustering. Cell *67*, 909–916.

Campanelli, J.T., Gayer, G.G., and Scheller, R.H. (1996). Alternative RNA splicing that determines agrin activity regulates binding to heparan and α-dystroglycan. Development *122*, 1663–1672.

Chang, D., Woo, J.S., Campanelli. J., Scheller, R.H., and Ignatius, M.J. (1997). Agrin inhibits neurite outgrowth but promotes attachment of embryonic motor and sensory neurons. Dev. Biol. *181*, 21–35.

Chomczynski, P., and Sacchi, N. (1987). Single-step method of RNA isolation by acid guanidinium thiocyanate-phenol-chloroform extraction. Anal. Biochem. *162*, 156–159.

Cohen, I., Rimer, M., Lomo, T., and McMahan, U.J. (1997a). Agrin-induced postsynaptic-like apparatus in skeletal muscle fibers *in vivo*. Mol. Cell. Neurosci. *9*, 237–253.

Cohen, N.A., Kaufmann, W.E., Worley, P.F., and Rupp, F. (1997b). Expression of agrin in the developing and adult rat brain. Neuroscience *76*, 581–596.

Covault, J., Cunningham, J.M., and Sanes, J.R. (1987). Neurite outgrowth on cryostat sections of innervated and denervated skeletal muscle. J. Cell Biol. *105*, 2479–2488.

Dai, Z., and Peng, H.B. (1996). From neurite to nerve terminal: induction of presynaptic differentiation by target-derived signals. Semin. Neurosci. *8*, 97–106.

DeChiara, T., Bowen, D.C., Valenzuela, D.M., Simmons, M.V., Poueymirou, W.T., Thomas, S., Kinetz, E., Smith, C., Compton, D.L., Park, J.S., et al. (1996). The receptor tyrosine kinase MuSK is required for neuromuscular junction formation in vivo. Cell *85*, 501–512.

Denzer, A.J., Brandenberger, R., Gesemann, M., Chiquet, M., and Ruegg, M.A. (1997). Agrin binds to the nerve–muscle basal lamina via laminin. J. Cell Biol. *137*, 671–683.

Fallon, J.R., and Gelfman, C.E. (1989). Agrin-related molecules are concentrated at acetylcholine receptor clusters in normal and aneural developing muscle. J. Cell Biol. *108*, 1527–1535.

Ferns, M., Hoch, W., Campanelli, J.T., Rupp, F., Hall, Z.W., and Scheller, R.H. (1992). RNA splicing regulates agrin-mediated acetylcholine receptor clustering activity in cultured myotubes. Neuron *8*, 1079–1086.

Ferns, M., Campanelli, J.T., Hoch, W., Scheller, R.H., and Hall, Z.M. (1993). The ability of agrin to cluster AChRs depends on alternative splicing and on cell surface proteoglycans. Neuron *11*, 491–502.

Gautam, M., Noakes, P.G., Moscoso, L.M., Rupp, F., Scheller, R.H., Merlie, J.P., and Sanes, J.R. (1996). Defective neuromuscular synaptogenesis in agrin-deficient mutant mice. Cell *85*, 525–535.

Gesemann, M., Denzer, A.J., and Ruegg, M.A. (1995). Acetylcholine receptor–aggregating activity of agrin isoforms and mapping of the active site. J. Cell Biol. *128*, 625–636.

Gesemann, M., Cavalli, V., Denzer, A.J., Brancaccio, A., Schumacher, B., and Ruegg, M.A. (1996). Alternative splicing of agrin alters its binding to heparan, dystroglycan, and the putative agrin receptor. Neuron *16*, 755–767.

Godfrey, E.W., Siebenlist, R.E., Wallskog, P.A., Walters, L.M., Bolender, D.L., and Yorde, D.E. (1988). Basal lamina components are concentrated in premuscle masses and at early acetylcholine receptor clusters in chick embryo hindlimb muscles. Dev. Biol. *130*, 471–486.

Halfter, W., Schurer, B., Yip, J., Yip, L., Tsen, G., Lee, J.A., and Cole, G.J. (1997). Distribution and substrate properties of agrin, a heparan sulfate proteoglycan of developing axonal pathways. J. Comp. Neurol. *383*, 1–17.

Hirano, Y., and Kidokoro, Y. (1989). Heparin and heparan sulfate partially inhibit induction of acetylcholine receptor accumulation by nerve in *Xenopus* culture. J. Neurosci. *9*, 1555–1561.

Hoch, W., Ferns, M., Campanelli, J.T., Hall, Z.W., and Scheller, R.H. (1993). Developmental regulation of highly active alternatively spliced forms of agrin. Neuron *11*, 479–490.

Hoch, W., Campanelli, J.T., Harrison, S., and Scheller, R.H. (1994). Structural domains of agrin required for clustering of nicotinic acetylcholine receptors. EMBO J. *13*, 2814–2821.

Hopf, C., and Hoch, W. (1997). Heparan inhibits acetylcholine receptor aggregation at two distinct steps in the agrin-induced pathway. Eur. J. Neurosci. *9*, 1170–1177.

Jones, G., Herczeg, A., Ruegg, M.A., Lichtsteiner, M., Kroger, S., and Brenner, H.R. (1996). Substrate-bound agrin induces expression of acetylcholine receptor epsilon-subunit gene in cultured mammalian muscle cells. Proc. Natl. Acad. Sci. USA *93*, 5985–5990.

Jones, G., Meier, T., Lichtsteiner, M., Witzemann, V., Sakmann, B., and Brenner, H.R. (1997). Induction by agrin of ectopic and functional postsynaptic-like membrane in innervated muscle. Proc. Natl. Acad. Sci. USA *94*, 2654–2659.

Lewandoski, M., and Martin, G.R. (1997). Cre-mediated chromosome loss in mice. Nat. Genet. *17*, 223–225.

Li, Z., Massengill, J.L., O'Dowd, D.K., and Smith, M.A. (1997). Agrin gene expression in mouse somatosensory cortical neurons during development *in vivo* and in cell culture. Neuroscience *79*, 191–201.

Lupa, M.T., Gordon, H., and Hall, Z.W. (1990). A specific effect of muscle cells on the distribution of presynaptic proteins in neurites and its absence in a C2 muscle cell variant. Dev. Biol. *142*, 31–43.

Martin, P.T., and Sanes, J.R. (1997). Integrins mediate adhesion to agrin and modulate agrin signaling. Development *124*, 3909–3917.

McMahan, U.J. (1990). The agrin hypothesis. Cold Spring Harbor Symp. Quant. Biol. *55*, 407–418.

McMahan, U.J., Horton, S.E., Werle, M.J., Honig, L.S., Kroger, S., Ruegg, M.A., and Escher, G. (1992). Agrin isoforms and their role in synaptogenesis. Curr. Opin. Cell Biol. *4*, 869–874.

Meier, T., Hauser, D.M., Chiquet, M., Landmann, L., Ruegg, M.A., and Brenner, H.R. (1997). Neural agrin induces ectopic postsynaptic specializations in innervated muscle fibers. J. Neurosci. *17*, 6534–6544.

Meier, T., Masciulli, F., Moore, C., Schoumacher, F., Eppenberger, U., Denzer, A.J., Jones, G., and Brenner, H.R. (1998a). Agrin can mediate acetylcholine receptor gene expression in muscle by aggregation of muscle-derived neuregulins. J. Cell Biol. *141*, 715–726.

Meier, T., Ruegg, M.A., and Wallace, B.G. (1998b). Muscle-specific agrin isoforms reduce phosphorylation of AChR γ and δ subunits in cultured muscle cells. Mol. Cell. Neurosci. *11*, 206–216.

Mook-Jung, I., and Gordon, H. (1996). Acetylcholine receptor clustering associates with proteoglycan biosynthesis in C2 variant and heterkaryon muscle cells. J. Neurobiol. *31*, 210–218.

Nagy, A., Rossant, J., Nagy, R., Abromow-Newerly, W., and Roder, J.C. (1993). Derivation of completely cell culture–derived mice from early-passage embryonic stem cells. Proc. Natl. Acad. Sci. USA *90*, 8424–8428.

Noakes, P.G., Gautam, M., Mudd, J., Sanes, J.R., and Merlie, J.P. (1995). Aberrant differentiation of neuromuscular junctions in mice lacking s-laminin/laminin β2. Nature *374*, 258–262.

O'Connor, L.T., Lauterborn, J.C., Gall, C.M., and Smith, M.A. (1994). Localization and alternative splicing of agrin mRNA in adult rat brain: transcripts encoding isoforms that aggregate acetylcholine receptors are not restricted to cholinergic neurons. J. Neurosci. *14*, 1141–1152.

O'Toole, J.J., Deyst, K.A., Bowe, M.A., Nastuk, M.A., McKechnie, B.A., and Fallon, J.R. (1996). Alternative splicing of agrin regulates its binding to heparan, α-dystroglycan, and the cell surface. Proc. Natl. Acad. Sci. USA *93*, 7369–7374.

Patton, B.L., Miner, J.H., Chiu, A.Y., and Sanes, J.R. (1997). Localization, regulation and function of laminins in the neuromuscular system of developing, adult and mutant mice. J. Cell Biol. *139*, 1507–1521.

Pin, C.L., Ludolph, D.C., Cooper, S.T., Klocke, B.J., Merlie, J.P., and Konieczny, S.F. (1997). Distal regulatory elements control MRF4 gene expression in early and late myogenic cell populations. Dev. Dynam. *208*, 299–312.

Porter, B.E., Weis, J., and Sanes, J.R. (1995). A motoneuron-selective stop signal in the synaptic protein S-laminin. Neuron *14*, 549–559.

Rimer, M., Mathiesen, I., Lomo, T., and McMahan, U.J. (1997). Gamma-AChR/epsilon-AChR switch at agrin-induced postsynaptic-like apparatus in skeletal muscle. Mol. Cell. Neurosci. *9*, 254–263.

Role, L.W., Matossian, V.R., O'Brien, R.J., and Fischbach, G.D. (1985). On the mechanism of acetylcholine receptor accumulation at newly formed synapses on chick myotubes. J. Neurosci. *5*, 2197–2204.

Ruegg, M.A., Tsim, K.W.K., Horton, S.E., Kroger, S., Escher, G., Gensch, E.M., and McMahan, U.J. (1992). The agrin gene codes for a family of basal lamina proteins that differ in function and distribution. Neuron *8*, 691–699.

Rupp, F., Ozcelik, T., Linial, M., Peterson, K., Francke, U., and Scheller, R.H. (1992). Structure and chromosomal localization of the mammalian agrin gene. J. Neurosci. *12*, 3535–3544.

Sanes, J.R., and Lichtman, J.W. (1999). Development of the vertebrate neuromuscular junction. Annu. Rev. Neurosci., in press.

Sauer, B. (1998). Inducible gene targeting in mice using the Cre/*lox* system. Methods Enzymol. *14*, 381–392.

Serpinskaya, A.S., Feng, G., Sanes, J.R., and Craig, A.M. (1999). Synapse formation between agrin mutant hippocampal neurons. Dev. Biol. *205*, 65–78.

Smith, M.A., and O'Dowd, D.K. (1994). Cell-specific regulation of agrin RNA splicing in the chick ciliary ganglion. Neuron *12*, 795–804.

Stone, D.M., and Nikolics, K. (1995). Tissue- and age-specific expression patterns of alternatively spliced agrin mRNA transcripts in embryonic rat suggest novel developmental roles. J. Neurosci. *15*, 6767–6778.

Sugiyama, J., Bowen, D.C., and Hall, Z.W. (1994). Dystroglycan binds nerve and muscle agrin. Neuron *13*, 103–115.

Valenzuela, D.M., Stitt, T.N., DiStefano, P.S., Rojas, E., Mattsson, K., Compton, D.L., Nunez, L., Park, J.S., Stark, J.L., Gies, D.R., et al. (1995). Receptor tyrosine kinase specific for the skeletal muscle lineage: expression in embryonic muscle, at the neuromuscular junction, and after injury. Neuron *15*, 573–584.

Wallace, B.G. (1990). Inhibition of agrin-induced acetylcholine-receptor aggregation by heparin, heparan sulfate, and other polyanions. J. Neurosci. *10*, 3576–3582.